Published in final edited form as:
Anal Chem. 2010 March 1; 82(5): 1975–1981. doi:10.1021/ac902725q.

Silicon Photonic Microring Resonators for Quantitative Cytokine Detection and T-Cell Secretion Analysis

Matthew S. Luchansky and **Ryan C. Bailey***
Department of Chemistry, Institute for Genomic Biology, and Micro and Nanotechnology Laboratory, University of Illinois at Urbana-Champaign, 600 South Mathews Avenue, Urbana, Illinois 61801

Abstract

The ability to perform multiple simultaneous protein biomarker measurements in complex media with picomolar sensitivity presents a large challenge to disease diagnostics and fundamental biological studies. Silicon photonic microring resonators represent a promising platform for real-time detection of biomolecules on account of their spectral sensitivity towards surface binding events between a target and antibody-modified microrings. For all refractive index-based sensing schemes the mass of bound analytes, in combination with other factors such as antibody affinity and surface density, contributes to the observed signal and measurement sensitivity. Therefore, proteins that are simultaneously low in abundance and have a lower molecular weight are often challenging to detect. By employing a more massive secondary antibody to amplify the signal arising from the initial binding event, it is possible to improve both the sensitivity and the specificity of protein assays, allowing for quantitative sensing in complex sample matrices. Herein, a sandwich assay is used to detect the 15.5 kDa human cytokine interleukin-2 (IL-2) at concentrations down to 100 pg/mL (6.5 pM) and to quantitate unknown solution concentrations over a dynamic range spanning 2.5 orders of magnitude. This same sandwich assay is then used to monitor the temporal secretion profile of IL-2 from Jurkat T lymphocytes in serum-containing cell culture media in the presence of the entire Jurkat secretome. The same temporal secretion analysis is performed in parallel using a commercial ELISA, revealing similar IL-2 concentration profiles but superior precision for the microring resonator sensing platform. Furthermore, we demonstrate the generality of the sandwich assay methodology on the microring resonator platform for the analysis of any biomolecular target for which two high affinity antibodies exist by detecting the ~8 kDa cytokine interleukin-8 (IL-8) with a limit of detection and dynamic range similar to that of IL-2. This work demonstrates the first application of silicon photonic microring resonators for detecting cellular secretion of cytokines and represents an important advance for the detection of protein biomarkers on an emerging analytical platform.

Introduction

Optical biosensors based on refractive index (RI) changes that accompany analyte binding have garnered attention for their potential to conduct biological assays without fluorescent or enzymatic labels, which can increase cost and complexity, add heterogeneity, and perturb native binding interactions.[1, 2] Within the category of RI-based optical biosensors, microcavity resonators have recently been shown to be promising platforms for label-free biomolecular detection. Examples of microcavity resonators include microtoroids,[3] microspheres,[4, 5] liquid-

baileyrc@illinois.edu.

Supporting Information Available: Surface functionalization results, a sandwich assay negative control experiment, real-time calibration data for both IL-2 and IL-8, and ring resonator response and calibration data for the cell culture experiments are available in the supporting information. This material is available free of charge via the Internet at http://pubs.acs.org.

core capillaries,[6, 7] and microrings.[8, 9] Molecules that interact with the sensor surface through antigen-specific capture probes (antibodies, cDNA, etc.) increase the local refractive index near the microring, facilitating the observation of binding events in real time. We have previously described the operational principles of our microring detection platform.[10–12] Briefly, light is coupled into on-chip, linear Si waveguides that access the microrings. At particular wavelengths, photons circulating the microring constructively interfere with those propagating down the adjacent linear waveguide resulting in an optical resonance as defined by:

$$m\lambda = 2\pi r n_{eff}$$

where m is an integer, r is the microring radius, and n_{eff} is the effective refractive index. This resonance is measured as a drop in light intensity transmitted down the linear waveguide past the microring as the wavelength is modulated using a tunable laser. Biomolecule detection is achieved by monitoring shifts in the resonant wavelength on account of binding-induced changes in the local refractive index at the microring surface. The potential of ring resonators has recently been demonstrated in biologically relevant systems, including the detection of proteins,[10, 13, 14] nucleic acids,[15] phage particles,[16] and whole cells.[17] Our group is particularly interested in silicon-on-insulator microring optical resonators, which are constructed by widely-used semiconductor fabrication techniques and thus are amenable to the incorporation of many discrete sensing elements onto a single millimeter-scale chip.[11, 12] Previously, we described the use of a newly designed analytical platform for the sensitive quantitation of protein biomarkers[10, 18] and nucleic acids.[11]

Cytokines, which are cell-signaling proteins secreted by lymphocytes and epithelial cells, represent a class of protein targets that are particularly challenging to detect in complex samples with label-free biosensors due to their small size and relatively low abundance. Cytokines mediate human immune response and are involved in inflammation and cell proliferation processes through a complex network of cytokine secretion and cellular recognition.[19] Furthermore, they are prospective biomarkers for many diseases, including prostate,[20] breast,[21] and throat cancers,[22] as well as a variety of autoimmune and inflammatory diseases.[23] Broad interest exists in developing sensitive cytokine analysis platforms, as evidenced by notable recent reports describing fluorescent fiber-optic microsphere arrays,[24] microdevices for T-cell capture and fluorescence-based cytokine measurements,[25] and optofluidic 1-D photonic-crystal-based sensors.[26]

Interleukin-2 (IL-2), also known as T-cell growth factor, is a 15.5 kDa cytokine produced by T lymphocytes that is responsible for T-cell proliferation.[27] IL-2 levels are correlated with the relative degree of T-cell activation or inhibition, which in turn serve as a general gauge of immune responsiveness. Therefore, IL-2 levels have been used as an indicator of antiretroviral response in HIV patients[28] and immune system health following chemotherapy,[29] in addition to other diagnostic and prognostic applications. Jurkat cells, a well-characterized human cancer cell line derived from a childhood leukemia patient, are often used as a model to study T-cell activation or inhibition *in vitro*.[30, 31] Jurkat T-cells are known to secrete IL-2 upon mitogenic stimulation with phorbol esters and either lectins or monoclonal antibodies against the T3 antigen[32] and thus serve as a suitable *in vitro* model system for validation of new cytokine detection platforms. Herein, we demonstrate the quantitation of IL-2 secretion from Jurkat cells stimulated with the phorbol ester PMA and the lectin PHA. For comparison, an enzyme-linked immunosorbent assay (ELISA) is used to measure IL-2 concentrations in parallel, and the silicon photonic microring resonator sensing platform demonstrates the ability to quantify Jurkat secretion with greater precision and shorter incubation times. While beyond the scope of this paper, it is important to keep in mind that arrays of microring resonators could, in the

future, be utilized to simultaneously detect the levels of multiple cytokines from within a single sample volume. Therefore, this manuscript represents a key first step towards the development of a powerful immunological analysis platform.

In this report, we employ a secondary antibody in a sandwich assay format which allows for more sensitive detection of IL-2 in complex media. Though this assay no longer retains the distinction of being "label-free," a term commonly used to described biosensor techniques such as surface plasmon resonance, quartz crystal microgravimetry, and field effect transistors among others,[1] it still avoids limitations of cost and assay complexity associated with fluorescent, enzymatic, or radioactive tags.[33, 34] As has been previously demonstrated using surface plasmon resonance, secondary antibody binding increases both assay sensitivity and specificity in the detection of low-abundance proteins in complex samples.[22, 35, 36] Compared to the size of an antibody (~150 kDa), IL-2 is relatively small. Thus, its binding to the sensor surface generates a smaller increase in the refractive index, which leads to a smaller shift in resonance wavelength. By using a larger anti-IL-2 molecule in a secondary amplification step, the signal from IL-2 binding is effectively enhanced, as shown in Figure 1. The use of a secondary antibody not only lowers the limit of detection to 0.1 ng/mL, a level relevant for the analysis of cellular secretions, but also increases the specificity of the assay by providing an additional analyte recognition element.

Experimental Section

Materials

3-N-((6-(N′-Isopropylidene-hydrazino))nicotinamide)propyltriethyoxysilane (HyNic silane) and succinimidyl 4-formyl benzoate (S-4FB) were purchased from SoluLink (San Diego, CA). Monoclonal mouse anti-human IL-2 (capture antibody, catalog# 555051, clone 5344.111) and monoclonal biotin mouse anti-human IL-2 (detection antibody, catalog# 555040, clone B33-2), both in phosphate buffered saline (PBS) containing 0.09% sodium azide, were purchased from BD Biosciences (San Jose, CA). These served as the primary and secondary antibodies, respectively. Recombinant human IL-2 (catalog# 14-8029) in PBS (pH 7.2, with 150 mM NaCl and 1.0% BSA) was purchased from eBioscience (San Diego, CA). PBS was reconstituted in deionized water from Dulbecco's phosphate buffered saline packets purchased from Sigma-Aldrich (St. Louis, MO). Aniline was obtained from Acros Organics (Geel, Belgium). Phorbol 12-myristate 13-acetate (PMA, Product# P 1585) was purchased from Sigma-Aldrich and dissolved in dimethyl sulfoxide to 0.5 mg/mL. The lectin phytohemagglutinin (PHA-P) from *Phaseolus vulgaris* (Product# L 9132) was also purchased from Sigma-Aldrich and dissolved in PBS, pH 7.4 to 0.5 mg/mL. Zeba spin filter columns were obtained from Pierce (Rockford, IL). A human IL-2 enzyme linked immunosorbent assay kit (OptEIA™ ELISA Kit II, catalog# 550611) that includes the previously described antibody clones was purchased from BD Biosciences. Cell culture media, RPMI 1640 supplemented with 10% fetal bovine serum (FBS) and penicillin/streptomycin (100 U/mL each), was obtained from the School of Chemical Sciences Cell Media Facility at the University of Illinois at Urbana-Champaign. All other chemicals were obtained from Sigma-Aldrich and used as received.

All buffers and dilutions were made with purified water (ELGA PURELAB filtration system; Lane End, UK), and the pH was adjusted with either 1 M HCl or 1 M NaOH. Antibody immobilization buffer was 50 mM sodium acetate and 150 mM sodium chloride adjusted to pH 6.0. Capture antibody regeneration buffer was 10 mM glycine and 160 mM NaCl adjusted to pH 2.2. BSA-PBS buffer used for IL-2 sensor calibration and detection was made by dissolving solid bovine serum albumin (BSA) in PBS (pH 7.4) to a final concentration of 0.1 mg/mL. For blocking, 2% BSA (w/v) in PBS was used.

Silicon photonic microring resonator array chips and the instrumentation for microring resonance wavelength determination were designed in collaboration with and built by Genalyte, Inc. (San Diego, CA). These materials and instrumentation have been described previously.[10–12] Briefly, silicon microring substrates (6 × 6 mm) contain sixty-four microrings (30 μm diameter) that are accessed by linear waveguides terminated with input and output diffractive grating couplers, allowing independent determination of the resonance wavelength for each microring. Up to thirty-two microring sensors are monitored simultaneously, eight of which are used solely to control for thermal drift. The instrumentation employs computer-controlled mirrors and a tunable, external cavity diode laser (center frequency 1560 nm) to rapidly scan the chip surface and sequentially interrogate the array of microring resonators, allowing determination of resonance wavelength for each independent sensor with ~250 msec time resolution.

Functionalization of Silicon Photonic Microring Resonator Arrays

Prior to functionalizing the microring surfaces, sensor chips were cleaned by a 30-sec immersion in piranha solution (3:1 H_2SO_4: 30% H_2O_2)[37] followed by rinsing with copious amounts of water and drying in a stream of nitrogen gas. For all subsequent steps, sensor chips were loaded into a previously described custom cell with microfluidic flow channels defined by a Mylar gasket,[10] and flow was controlled via an 11 Plus syringe pump (Harvard Apparatus; Holliston, MA) operated in withdraw mode. Flow rates for functionalization and cytokine detection steps were set to 5 μL/min. The flow rate was set to 30 μL/min for all additional steps.

The chip was first exposed to a solution of 1 mg/mL HyNic silane in 95% ethanol and 5% dimethyl formamide (DMF) for 20 minutes to install a hydrazine moiety on the silicon oxide chip surface, followed by rinsing with 100% ethanol (Figure S-1, Figure S-2). In a separate reaction vial, the capture antibody was functionalized with an aldehyde moiety by reacting anti-IL-2 (0.5 mg/mL) with a 5-fold molar excess of 0.2 mg/mL S-4FB (dissolved first in DMF to 2 mg/mL for storage and diluted in PBS to 0.2 mg/mL) for 2 hrs at room temperature. After buffer-exchanging to remove excess S-4FB using Zeba spin filter columns and dilution to 0.1 mg/mL, the antibody-containing solution was flowed over the chip to allow covalent attachment to the hydrazine-presenting chip surface (Figure S-1, Figure S-3). Aniline (100 mM) was added to the antibody solution prior to flowing over the chip, serving as a catalyst for hydrazone bond formation[38, 39] that improves biosensor surface functionalization. The previously-described Mylar gasket[10] allows for selective antibody functionalization on 15 rings under fluidic control. After the coupling reaction, a low-pH glycine-based regeneration buffer rinse removed any non-covalently bound antibody. A final blocking step was carried out by exposing the sensor surface to a 2% solution (w/v) of BSA in PBS overnight.

Calibration of Sensors and Detection of IL-2

IL-2 calibration standards were prepared by serial dilution of recombinant human IL-2 (≥ 0.1 mg/mL) in BSA-PBS to the following concentrations: 50, 25, 10, 4, 1.6, 0.64, 0.26, 0.10, and 0 ng/mL. Blinded unknown samples were prepared independently from similar stocks. All sandwich assays performed on the chip surface were monitored in real time and involved a 30-min incubation (5 μL/min) in IL-2 standard or unknown solution followed by a 15-min read-out with the secondary detection anti-IL-2 antibody (2 μg/mL, 5 μL/min). A low-pH glycine buffer rinse, which disrupts non-covalent protein interactions, was used to regenerate the capture anti-IL-2 surface. The chip was blocked with BSA-PBS prior to subsequent IL-2 detection experiments.

Data Processing

The response from the detection antibody binding to captured IL-2 at the surface as a function of IL-2 concentration was used to calibrate the sensor response for each ring (n = 15 independent measurements). Prior to quantitation, the shift response of a control ring, which was not functionalized with capture anti-IL-2 antibody but was exposed to the same solution as the functionalized rings, was subtracted from each of the functionalized ring signals to account for any non-specific binding, as well as temperature or instrumental drift. The corrected secondary signal after 15 minutes of detection antibody incubation was measured as a net shift for each IL-2 standard and unknown, with the signal from each ring serving as an independent measure of IL-2 concentration. The average corrected secondary shift was plotted against concentration to obtain a calibration plot, which was then fit with a quadratic regression for quantitation of unknowns by inverse regression.

Jurkat Cell Culture, Stimulation, and Secretion Profiling

Jurkat T lymphocytes were passaged into fresh media at 10^6 cell/mL (10 mL culture in each of two T25 vented flasks). One flask was immediately stimulated to secrete IL-2 by adding the mitogens PMA (50 ng/mL) and PHA (2 μg/mL) using an established procedure,[31, 32, 40, 41] while the other flask served as a non-stimulated control. Both flasks were immediately returned to the cell culture incubator (37°C, 5% CO_2, 70% relative humidity). Aliquots (1 mL) were withdrawn from both the control and stimulated flasks at four time points: 0, 8, 16, and 24 hours post-stimulation. The cell culture aliquots were centrifuged at 1,000 RPM for 5 min to pellet the cells, and then the supernatant was removed and centrifuged at 10,000 RPM for 5 min to pellet any remaining cellular debris. Cell culture aliquots were divided into two identical tubes and stored for less than 24 hours at 4°C for subsequent parallel analysis by both ELISA and the microring resonator platform. A sensor chip was selectively functionalized with anti-IL-2 capture antibody as described above and calibrated to secondary antibody response with the following IL-2 standards prepared by serial dilution in cell culture media: 50, 20, 8, 3.2, and 1.3 ng/mL. Immediately after calibration, aliquots taken at each time point for both control and stimulated cells were flowed over all rings on the chip (30 min, 5 μL/min) followed by introduction of the detection anti-IL-2 (2 μg/mL, 15 min, 5 μL/min). An IL-2 ELISA, conducted as per the manufacturer's instructions, was performed on the same samples from each time point for validation and comparison to results obtained from the microring resonator platform.

Results and Discussion

The goal of this study is to establish the use of secondary antibodies to improve detection limits and increase sensor specificity for cytokine detection in complex media using a microring resonator platform. After demonstrating the utility of the sandwich assay technique for quantitative detection of IL-2 with picomolar sensitivity, the platform is applied to the temporal monitoring of IL-2 secretion from stimulated Jurkat T lymphocytes.

Sandwich Assay for Sensitive, Quantitative Cytokine Detection

The wavelengths of light that meet the microring resonance condition are extremely sensitive to the local refractive index. Therefore, biomolecular binding events that increase the effective refractive index at the sensor surface are observed as increase in the resonant wavelength of the microcavity. This shift in resonance wavelength is analyte concentration dependent and serves as the basis for all sensor calibration and unknown sample determination experiments. The silicon microring is passivated with native SiO_x, which allows for initial functionalization with a hydrazine-terminated silane in preparation for covalent antibody immobilization. All surface derivitization steps are monitored in real time as a shift in the resonance wavelength of each ring (See Figures S-2 and S-3 in the Supporting Information). Microfluidics are used to confine antibody functionalization to only 15 of the 24 active sensing rings, allowing the

other 9 rings to serve as controls for non-specific binding, bulk refractive index changes, and thermal drift as they are exposed to identical IL-2 standards and unknown samples.

Once the rings are functionalized with capture anti-IL-2, a 45-min IL-2 sandwich assay is performed, as shown in Figure 1. Initially, binding of the 15.5 kDa IL-2 to the capture antibody results in a small wavelength shift (~15 pm over 30 min for 50 ng/mL IL-2; hardly detectable for lower concentrations and incubation times). After this primary binding event, a secondary detection anti-IL-2 antibody that recognizes a different IL-2 epitope is allowed to bind. The binding of the detection antibody, increases the observed signal (~40 pm over 15 min). In the absence of IL-2, secondary antibody introduction elicits no measureable binding response (See Figure S-4 in the Supporting Information). While this microring resonator detection modality is, strictly speaking, a refractive index-sensitive technique, the observed change in effective refractive index at the sensor surface is proportional to analyte mass under the reasonable assumption that all proteins have an equivalent refractive index.[4, 5] Though the secondary anti-IL-2 is roughly ten times as massive as IL-2, only a 3- to 5-fold increase in signal is observed as secondary antibody saturation at the surface causes the signal to level off at high concentrations. We attribute this observation to the limited steric accessibility of secondary antibodies to all bound antigens. More specifically, the random immobilization of the primary antibodies via modified lysine residues leads to some orientations that, while capable of binding IL-2, do not present the antigen in a manner in which the secondary epitope can be accessed for subsequent secondary binding. For both the antigen and the detection antibody binding steps, the assay speed is limited by protein diffusion to the microrings. Though the 45-min total assay time reported herein is considerably shorter than the approximately 4-hr ELISA assay, we are working towards further reducing the time-to-result by utilizing more highly optimized fluid delivery systems.

Following the sandwich assay detection, the sensor surface is regenerated with a low-pH glycine buffer rinse that disrupts non-covalent protein-protein and protein-surface interactions. By removing all IL-2 and anti-IL-2 detection antibody, the capture anti-IL-2 is restored to its original state for subsequent assays. Upon returning to buffer, the resonance wavelength returns to baseline, indicating effective regeneration. The capture antibody can be regenerated 20–30 times without substantial loss in binding activity, allowing for the consecutive analysis of many standards and samples on a single chip. In order to demonstrate the quantitative sensing capabilities of the platform, IL-2 sandwich assays were performed on nine calibration standards and two unknowns in BSA-PBS. Figure 2 shows the response for one representative sensor ring (out of 15 total) as a function of time for 11 consecutive sample exposures, IL-2 detection experiments, and surface regenerations. For purposes of quantitation, the shift associated with detection antibody binding after 15 min of exposure was measured. Though primary IL-2–capture antibody interactions are not easily observed at sub-ng/mL concentrations, the secondary amplification step allows a 0.10 ng/mL (6.5 pM) solution to be readily discerned from baseline.

The shift in resonance wavelength for each of 15 rings is measured independently of all other rings. This multiplexing capability, here applied to a single parameter assay, greatly reduces the time required to obtain statistically relevant measured values. In other words, redundant measurements are generated in parallel rather than consecutively, which reduces both assay time and sample consumption. These 15 independent measurements have the advantage of decreasing the inherent uncertainty of the assay, which adds to its quantitative utility. For sensor array calibration, the average secondary antibody binding response for all 15 rings is plotted against IL-2 concentration, as shown in Figure 3. The calibration plot is fitted with a quadratic regression ($R^2 = 0.999$) since, as expected, it is observed that the secondary signal begins to saturate at higher IL-2 concentrations (beyond 25 ng/mL) due to a limited number of accessible antibody binding sites. As the concentration approaches 50 ng/mL, a maximum secondary

signal (32.5 ± 3.6 pm, 95% CI, n = 15 rings) is reached. Linear regression can also be applied to the data between 0.1 and 4 ng/mL IL-2, yielding a slope of 1.56 Δpm per ng/mL (See Figure S-5 in the Supporting Information) that is in strong agreement with the quadratic regression (Figure 3).

Using this calibration curve, the concentrations of IL-2 in two blinded unknown samples (Unknown A and Unknown B) were determined to be 0.40 ± 0.21 and 7.73 ± 0.80 ng/mL, respectively. Reported uncertainties in both cases represent the 95% confidence interval for 15 independent measurements. Importantly, these values are in excellent agreement with the as prepared values of 0.37 ng/mL and 7.64 ng/mL for Unknowns A and B, respectively. The ability to accurately determine IL-2 concentrations over a broad concentration range (0.10 to 25 ng/mL) demonstrates the utility of sandwich assays on a microring resonator platform for protein quantitation.

To demonstrate the generality of the approach, we also successfully applied the sandwich assay methodology to detect another cytokine, IL-8, with similar sub-ng/mL sensitivity and comparable saturation behavior (See Figure S-6 in the Supporting Information). Similarly to IL-2, the calibration data is best fit with a quadratic function that can be used to determine IL-8 at concentrations between 0.1 and 20 ng/mL. Beyond cytokines, the sandwich assay detection method described herein is expected to be generally applicable to analysis of any biomolecule for which a high-affinity antibody pair exists.

IL-2 Detection and Quantitation in Complex Media

Building upon the calibration and unknown quantitation successes in buffer, we validated the sandwich assay approach for analysis in a more complex medium, specifically the detection of IL-2 in cell culture media. The media of interest, supplemented RPMI 1640, contains a wide variety of inorganic salts, amino acids, vitamins, antibiotics, and sugars at concentrations in the μg/mL – mg/mL range. Furthermore, the addition of fetal bovine serum, which contains a variable amount of total protein (ranging from 30–50 mg/mL),[42] adds to the complexity of the analysis. A final potentially complicating factor is the multitude of biomolecules (proteins and carbohydrates) secreted by the Jurkat cells into the surrounding media that are not necessarily the subject of the assay being performed. Clearly, assays performed within complex environments such as culture media require high specificity in order to detect a single protein species at sub-ng/mL levels in a variable matrix containing electrolytes, sugars, and other proteins in excess of mg/mL concentrations.

Prior to performing IL-2 detection in the Jurkat secretome, calibration was performed using IL-2 standards prepared in cell culture media. As in the previously described calibration, standards were prepared by serial dilution and flowed over the chip under conditions identical to those for detection in buffer. Sandwich assays were performed and monitored in real time (See Figure S-7 in the Supporting Information), and calibration was performed with five standard solutions over a concentration range relevant for subsequent cell culture analysis. The resulting calibration plot generated from secondary antibody-based detection was again fit with a quadratic function ($R^2 = 0.999$, See Figure S-8 in the Supporting Information). In comparing the calibration in buffer (Figure 3) to that in cell culture media (Figure S-8), we find that the response sensitivity decreases by a factor of ~2; however, sensitivity in the low ng/mL range is retained, enabling the monitoring of cytokine secretion from Jurkat T lymphocytes, a common model of immune response, as described below.

Jurkat IL-2 Secretion Analysis and Validation

A temporal secretion analysis was performed on freshly passaged Jurkat T cells (~10^6 cells/mL) by sampling the cell culture media at defined time points over a 24-hr period. The secretion

analysis was performed in parallel on both non-stimulated (control) cells and PMA/PHA-stimulated cells. After removing cells and cellular debris by centrifugation, the raw cell culture media-based samples were flowed across a single calibrated chip to maximize consistency in sensor response and accuracy in IL-2 concentration determination. A bulk RI change was observed upon the addition of cell media aliquots on account of differences in ionic strength between sterile media used in calibration and media which had supported Jurkat cell growth (See Figure S-9 in the Supporting Information). After a 30-min incubation in the Jurkat secretion aliquot, the secondary antibody response was measured and used to determine the IL-2 concentration according to the previous calibration relation (Figure S-8). Control rings were used to subtract the sensor response that arose from non-specific binding of Jurkat secretion proteins. After each sandwich assay was performed, the surface was regenerated and allowed to equilibrate for 20–30 minutes in sterile RPMI 1640 + 10% FBS to ensure effective capture antibody blocking prior to introducing subsequent Jurkat secretome samples.

The Jurkat secretion analysis revealed a pronounced difference in secreted IL-2 levels between stimulated and non-stimulated cells, as shown in Figure 4. Non-stimulated cells did not produce measureable levels of IL-2, but PMA/PHA-stimulated Jurkat cells showed an accumulation of IL-2 up to 15 ± 2 ng/mL (95% CI, n = 15) after 24 hours. This data is supported by literature reports that have demonstrated the absence of IL-2 transcripts and protein without stimulation[43, 44] as well as the synergistic effects of PMA and PHA, which must be added concurrently to stimulate IL-2 secretion.[32, 40] Previous reports describe IL-2 levels of 15–20 ng/10^6 cells from stimulated Jurkats under the culture conditions employed herein,[41, 45] consistent with microring resonator assay determinations.

In addition to using the microring resonator platform, the secretion analysis was performed in parallel with an IL-2 ELISA for further validation. The ELISA utilized herein was obtained from the same vendor (BD Biosciences) as the individual capture and secondary antibodies used in the microring resonator determination, and therefore serves as a valuable comparison given that identical antibody clones were used in both assays. Figure 4 shows the strong agreement, both qualitatively and quantitatively, in the IL-2 values measured using the ELISA kit and the microring resonator platform. The ELISA, performed on the same Jurkat secretion media aliquots assayed using microrings, gave a similar final IL-2 concentration after 24 hours of 21 ± 5 ng/mL (95% CI, n = 3). Additionally, a steady increase in accumulated IL-2 levels over time is observed for both techniques, further validating the quantitative potential of the sandwich assays performed on the microring resonator detection platform.

Though the two assays show strong agreement in average IL-2 levels at each time point, the ring resonator sandwich assay exhibits greater precision, as is evidenced by smaller uncertainties associated with the data points in Figure 4. Notably, the redundant, simultaneous multiplexing of the IL-2 assay on the microring sensor array (n = 15) reduces uncertainty in the determined concentration. Sample and reagent requirements generally limit ELISAs to triplicate analyses. Thus, the ability to perform many measurements from a single sample without requiring additional reagents or rinsing steps is a clear advantage for the silicon photonic microring resonator bioanalysis technique.

Conclusions

Sandwich assays performed on a silicon photonic microring resonator biosensor platform have been demonstrated as a highly quantitative tool for protein detection with sub-ng/mL sensitivity. This technique is capable of performing precise analyses in complex media, including cell culture secretions that include 10% serum and other additives. Sensitive determination of the cytokine IL-2 was demonstrated, with a limit of detection that is useful for performing a highly resolved temporal analysis of Jurkat T-cell secretion. This result was

validated with ELISA, and comparison between the techniques revealed superior precision for the microring detection platform. The ability to simultaneously perform precise measurements of low molecular mass and low abundance proteins on a scalable bioanalysis platform may allow multiplexed assays in which the measurements of multiple cytokines are integrated onto a single silicon photonic sensor array, and this manuscript represents an important first step towards this goal.

Supplementary Material

Refer to Web version on PubMed Central for supplementary material.

Acknowledgments

This work is funded by the NIH Director's New Innovator Award Program, part of the NIH Roadmap for Medical Research, through grant number 1-DP2-OD002190-01, and by the Camille and Henry Dreyfus Foundation. MSL is supported via a National Science Foundation Graduate Research Fellowship and a Robert C. and Carolyn J. Springborn Fellowship from the Department of Chemistry at the University of Illinois at Urbana-Champaign. We acknowledge Adam Washburn for his assistance in preparing the IL-2 unknown solutions and for offering many helpful comments.

References

1. Qavi AJ, Washburn AL, Byeon JY, Bailey RC. Anal Bioanal Chem 2009;394:121–135. [PubMed: 19221722]
2. Fan X, White IM, Shopova SI, Zhu H, Suter JD, Sun Y. Anal Chim Acta 2008;620:8–26. [PubMed: 18558119]
3. Armani AM, Kulkarni RP, Fraser SE, Flagan RC, Vahala KJ. Science 2007;317:783–787. [PubMed: 17615303]
4. Arnold S, Khoshsima M, Teraoka I, Holler S, Vollmer F. Opt Lett 2003;28:272–274. [PubMed: 12653369]
5. Vollmer F, Arnold S, Keng D. Proc Natl Acad Sci U S A 2008;105:20701–20704. [PubMed: 19075225]
6. White, IM.; Zhu, H.; Suter, JD.; Fan, X.; Zourob, M. Methods Mol Biol. Rasooly, A.; Herold, KE., editors. Vol. 503. Humana Press; New York, NY: 2009. p. 139-165.
7. Shopova SI, White IM, Sun Y, Zhu H, Fan X, Frye-Mason G, Thompson A, Ja S-j. Anal Chem 2008;80:2232–2238. [PubMed: 18271605]
8. Xu DX, Densmore A, Delage A, Waldron P, McKinnon R, Janz S, Lapointe J, Lopinski G, Mischki T, Post E, Cheben P, Schmid JH. Opt Express 2008;16:15137. [PubMed: 18795053]
9. Chao CY, Fung W, Guo LJ. IEEE J Sel Top Quantum Electron 2006;12:134.
10. Washburn AL, Gunn LC, Bailey RC. Anal Chem 2009;81:9499–9506. [PubMed: 19848413]
11. Bailey, RC.; Washburn, AL.; Qavi, AJ.; Iqbal, M.; Gleeson, M.; Tybor, F.; Gunn, LC. San Jose, CA, USA. 2009; Proc. SPIE; p. 72200N-72206.
12. Iqbal, M.; Gleeson, MA.; Spaugh, B.; Tybor, F.; Gunn, WG.; Hochberg, M.; Baehr-Jones, T.; Bailey, RC.; Gunn, LC. IEEE J Sel Top Quantum Electron. 2010. in press
13. De Vos K, Girones J, Popelka S, Schacht E, Baets R, Bienstman P. Biosensors Bioelectron 2009;24:2528.
14. Zhu H, Dale PS, Caldwell CW, Fan X. Anal Chem 2009;81:9858–9865. [PubMed: 19911811]
15. Suter JD, White IM, Zhu H, Shi H, Caldwell CW, Fan X. Biosensors Bioelectron 2008;23:1003.
16. Zhu H, White IM, Suter JD, Zourob M, Fan X. Analyst 2008;133:356. [PubMed: 18299750]
17. Ramachandran A, Wang S, Clarke J, Ja SJ, Goad D, Wald L, Flood EM, Knobbe E, Hryniewicz JV, Chu ST, Gill D, Chen W, King O, Little BE. Biosensors Bioelectron 2008;23:939.
18. Washburn AL, Luchansky MS, Bowman AL, Bailey RC. Anal Chem 2010;82:69–72. [PubMed: 20000326]
19. Young, HA. Methods Mol Biol. Kozlov, SV., editor. Vol. 511. Humana Press; New York, NY: 2009. p. 85-105.

20. Fujita K, Ewing CM, Sokoll LJ, Elliott DJ, Cunningham M, Marzo AMD, Isaac WB, Pavlovich CP. The Prostate 2008;68:872–882. [PubMed: 18361406]
21. Chavey C, Bibeau F, Gourgou-Bourgade S, Burlinchon S, Boissiere F, Laune D, Roques S, Lazennec G. Breast Cancer Res 2007;9:R15. [PubMed: 17261184]
22. Yang CY, Brooks E, Li Y, Denny P, Ho CM, Qi FX, Shi WY, Wolinsky L, Wu B, Wong DTW, Montemagno CD. Lab Chip 2005;5:1017–1023. [PubMed: 16175255]
23. O'Hara JRM, Benoit SE, Groves CJ, Collins M. Drug Discov Today 2006;11:342–347. [PubMed: 16580976]
24. Blicharz TM, Siqueira WL, Helmerhorst EJ, Oppenheim FG, Wexler PJ, Little FF, Walt DR. Anal Chem 2009;81:2106–2114. [PubMed: 19192965]
25. Zhu H, Stybayeva G, Macal M, Ramanculov E, George MD, Dandekar S, Revzin A. Lab Chip 2008;8:2197–2205. [PubMed: 19023487]
26. Mandal S, Goddard JM, Erickson D. Lab Chip 2009;9:2924–2932. [PubMed: 19789745]
27. Smith KA. Science 1988;240:1169–1176. [PubMed: 3131876]
28. Orsilles MA, Pieri E, Cooke P, Caula C. APMIS 2006;114:55–60. [PubMed: 16499662]
29. Mazur B, Mertas A, Sonta-Jakimczyk D, Szczepanski T, Janik-Moszant A. Hematol Oncol 2004;22:27–34. [PubMed: 15152368]
30. Sundrud MS, Torres VJ, Unutmaz D, Cover TL. Proc Natl Acad Sci U S A 2004;101:7727–7732. [PubMed: 15128946]
31. Gebert B, Fischer W, Weiss E, Hoffmann R, Haas R. Science 2003;301:1099–1102. [PubMed: 12934009]
32. Weiss A, Wiskocil R, Stobo J. J Immunol 1984;133:123–128. [PubMed: 6327821]
33. Kodadek T. Chem Biol 2001;8:105–115. [PubMed: 11251285]
34. Sun YS, Landry JP, Fei YY, Zhu XD, Luo JT, Wang XB, Lam KS. Langmuir 2008;24:13399–13405. [PubMed: 18991423]
35. Arima, Y.; Teramura, Y.; Takiguchi, H.; Kawano, K.; Kotera, H.; Iwata, H. Biosensors and Biodetection. 2009. p. 3-20.
36. Jang HS, Park KN, Kang CD, Kim JP, Sim SJ, Lee KS. Opt Commun 2009;282:2827–2830.
37. Caution! Piranha solutions are extraordinarily dangerous, reacting explosively with trace quantities of organics.
38. Dirksen A, Dawson PE. Bioconj Chem 2008;19:2543–2548.
39. Byeon, JY.; Limpoco, FT.; Bailey, RC. Unpublished work. 2010.
40. Manger B, Hardy KJ, Weiss A, Stobo JD. J Clin Invest 1986;77:1501–1506. [PubMed: 2422208]
41. Sigma-Aldrich . Cat# P1585 Datasheet. 2002. http://www.sigmaaldrich.com
42. Invitrogen. Cat# 26140. 2009. http://tools.invitrogen.com/content/sfs/productnotes/F_FBS%20Qualified%20RD-MKT-TL-HL0506021.pdf
43. Durand D, Bush M, Morgan J, Weiss A, Crabtree G. J Exp Med 1987;165:395–407. [PubMed: 3102668]
44. Kronke M, Leonard W, Depper J, Greene W. J Exp Med 1985;161:1593–1598. [PubMed: 2989408]
45. Rockwell CE, Raman P, Kaplan BLF, Kaminski NE. Biochem Pharmacol 2008;76:353–361. [PubMed: 18571623]

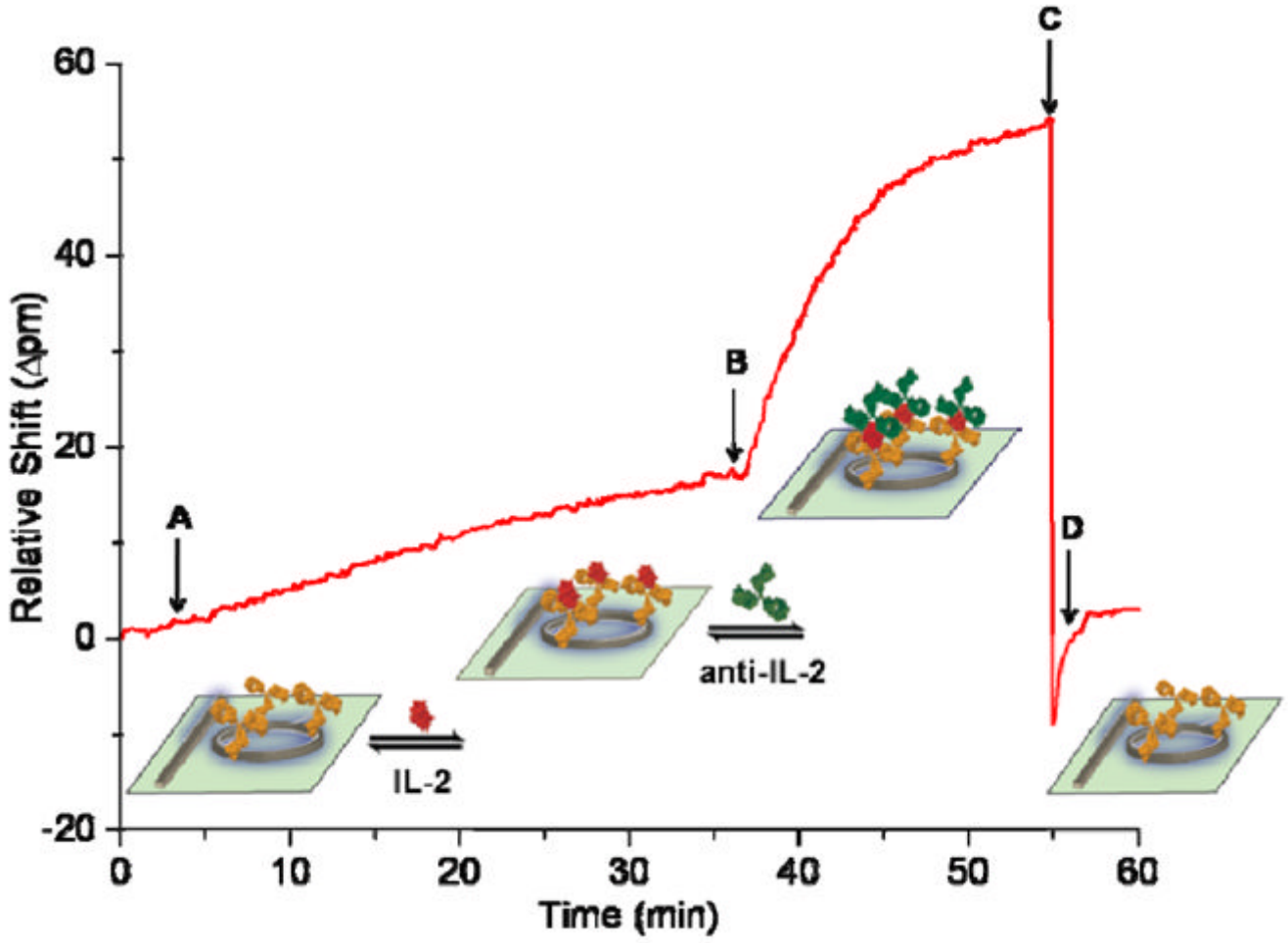

Figure 1.

Representative sandwich assay response and schematic for a single microring optical resonator functionalized with capture anti-IL-2 antibody. An anti-IL-2 antibody-modified microring resonator is initially incubated in buffer (time before **A**), then a 50 ng/mL solution of IL-2 is introduced to the ring (**A**) resulting in a ~15 pm net shift in resonance wavelength after 30 min of binding. Quantitative signal enhancement is then achieved by introducing an anti-IL-2 detection antibody (**B**), which gives a ~40 pm net shift in resonance wavelength after a 15 min incubation. The sensor is regenerated with a low-pH buffer rinse (**C**) prior to returning to buffer (**D**) for subsequent IL-2 analyses.

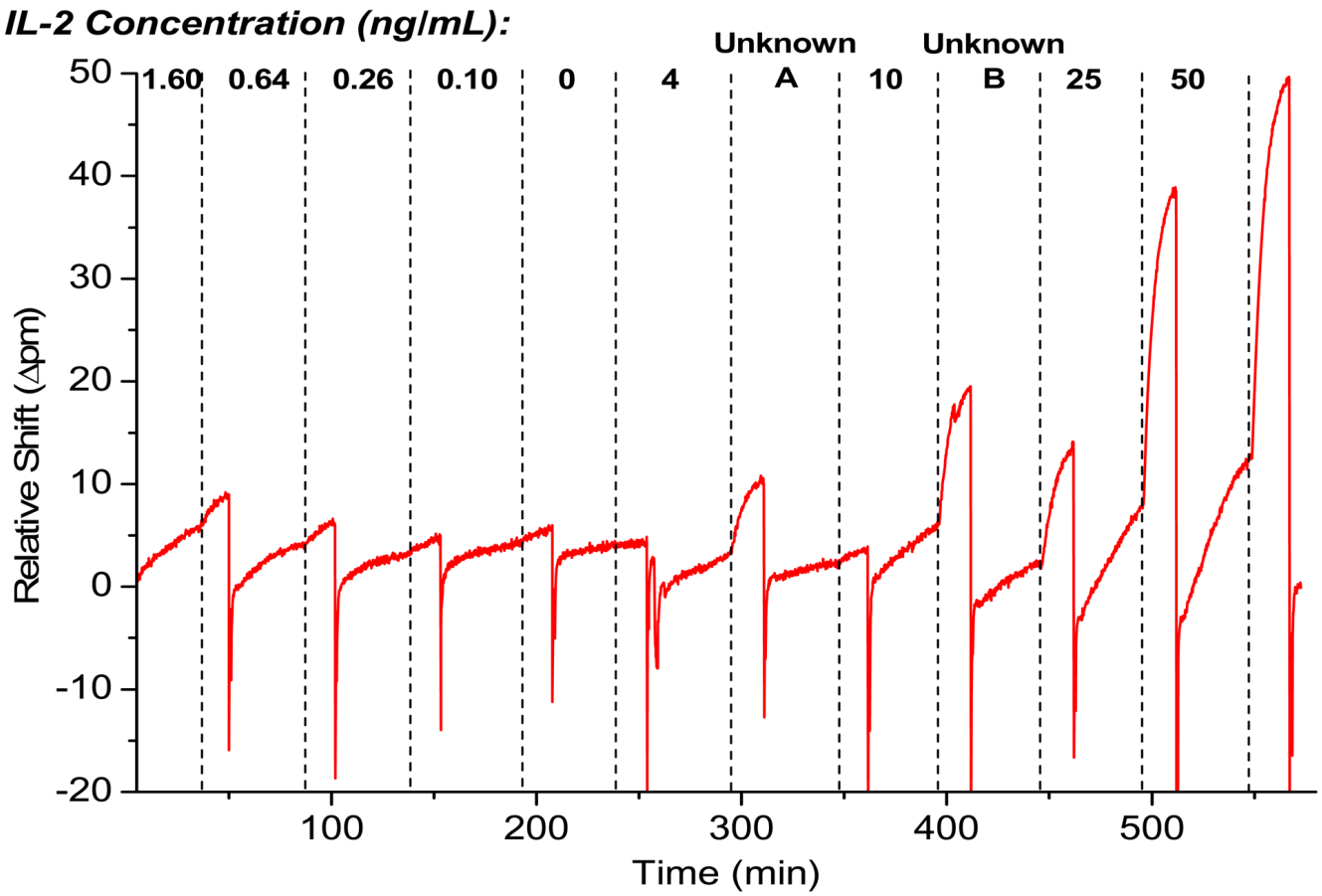

Figure 2.

Real-time monitoring of resonance wavelength shifts of an anti-IL-2 antibody-functionalized microring during exposure to a variety of known (0, 0.10, 0.26, 0.64. 1.60, 4, 10, 25, and 50 ng/mL) and two unknown solutions (Unknowns A and B) in BSA-PBS. Following a 30-min exposure to each IL-2 concentration, anti-IL-2 detection antibody is flowed over the ring (dashed lines), and the secondary net shift after 15 minutes is used for quantitation. A BSA-PBS sample without IL-2 produced no secondary anti-IL-2 binding signal, as shown between time points 238 and 253 minutes. After each secondary detection, the microring surface is regenerated by a low-pH glycine rinse, and the sample chamber returned to BSA-PBS to achieve a stable baseline before subsequent sample injections. The signal is corrected for drift by subtracting the shift from an adjacent control ring that is not functionalized with anti-IL-2 but is introduced to identical conditions throughout.

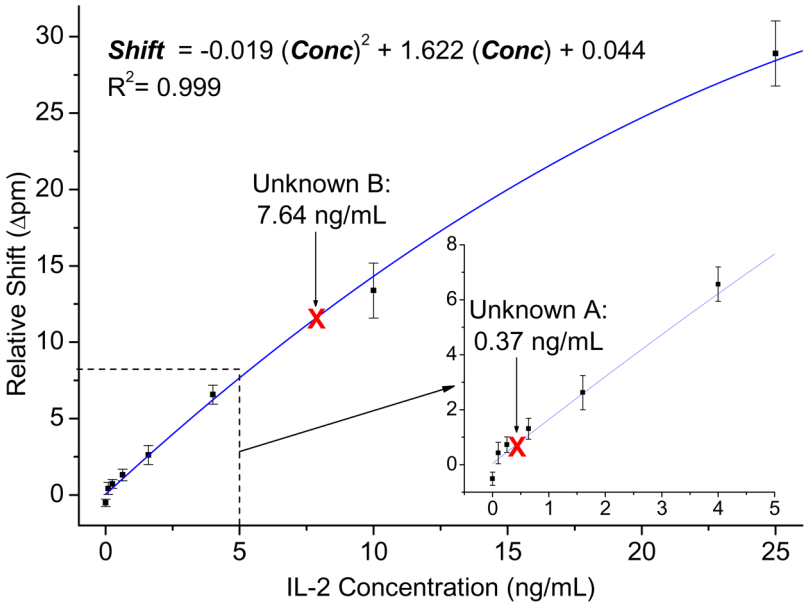

Figure 3.

Concentration-response plot of the average control-ring-corrected net shift as a function of IL-2 concentration, as determined from 15 microring resonators. Following 30-min incubation in IL-2 standard solutions prepared in BSA-PBS, the net shift arising from detection antibody binding is measured after 15 min for each ring. The plot is fit with a quadratic regression, and the displayed equation is used to successfully quantitate solutions with unknown IL-2 concentrations (relative positions of unknowns depicted on curve with red X). The inset in the lower right corner is an expanded view of the low concentration range below 4 ng/mL. Error bars represent the 95% confidence interval, n = 15 rings.

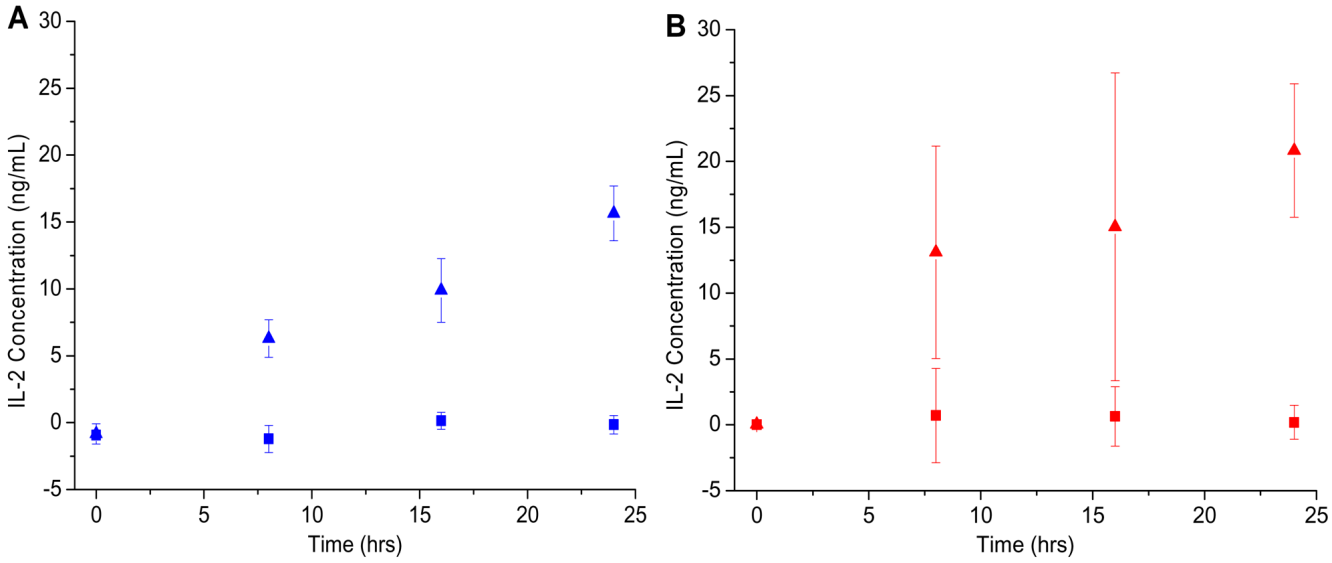

Figure 4.

Temporal Jurkat IL-2 secretion profile. Aliquots were taken at 8-hr intervals over a 24-hr period to compare IL-2 secretion from non-stimulated (squares) and PMA/PHA-stimulated (triangles) Jurkat T-cells. Results were obtained in parallel by using the microring resonator sandwich assay (**A**) and an IL-2 ELISA (**B**). Error bars represent the 95% confidence interval for n = 15 (**A**) and n = 3 (**B**).